Available online at www.sciencedirect.com
SCIENCE DIRECT®
Estuarine, Coastal and Shelf Science 68 (2006) 305–316
ESTUARINE COASTAL AND SHELF SCIENCE
www.elsevier.com/locate/ecss

Identification and characterisation of two optical water types in the Irish Sea from in situ inherent optical properties and seawater constituents

David McKee*, Alex Cunningham

SUPA, Physics Department, University of Strathclyde, 107 Rottenrow, Glasgow G4 0NG, Scotland

Received 20 December 2005; accepted 21 February 2006
Available online 18 April 2006

Abstract

This paper examines relationships between the inherent optical properties (IOPs) of the Irish Sea and concentrations of optically significant constituents, measured as chlorophyll (Chl), mineral suspended solids (MSS) and coloured dissolved organic material (CDOM). In situ measurements of IOPs at 98 stations fell into two groups with distinct characteristics. Instances include the ratio of particulate backscattering to non-water absorption at 676 nm ($b_{bp}676/a_n676$), the ratio of the non-water absorption coefficients at 440 nm and 676 nm (a_n440/a_n676) and the ratio of particulate scattering to non-water absorption (b_p/a_n) at 676 nm. The two groups showed corresponding differences in the proportions of their constituent concentrations with Chl/MSS values typically above 0.4 mg g^{-1} for stations with $b_{bp}676/a_n676 < 0.33$ and below 0.4 mg g^{-1} for stations with $b_{bp}676/a_n676 > 0.33$. CDOM concentrations showed no significant differences between groups. The occurrence of correlated groups in the IOP and constituent concentration data indicates the existence of identifiable sub-types of coastal water within the conventional Case 2 classification whose optical characteristics were dominated either by phytoplankton or suspended minerals. By applying linear regression analysis to the two groups we derived effective material-specific IOPs for these natural particle assemblages. The coefficients obtained enabled the successful reconstruction of total absorption, scattering and backscattering coefficients for a given water body from measurements of Chl, MSS and CDOM. This procedure may be useful for assimilating measurements of seawater composition into bio-optical models in shelf seas.

Keywords: optical properties; light absorption; light scattering; shelf seas; Irish Sea

1. Introduction

Radiative transfer modelling provides a systematic means of determining the effect of changes in the optical properties of seawater on underwater light fields and remote sensing reflectance signals (Kirk, 1981; Sathe and Sathyendranath, 1992; Mobley, 1994). In recent years, the combination of commercially available software such as Hydrolight (Sequoia) and new in situ sensors for measuring inherent optical properties has enabled greatly improved radiative transfer models to be constructed (Chang et al., 2003; McKee et al., 2003; Bulgarelli et al., 2003). These models are valuable tools for developing algorithms for interpreting ocean colour signals and formulating spectrally resolved models of primary productivity (Sathyendranath et al., 1989; Smith et al., 1989). However, systematic studies of the optical effects of phytoplankton, minerals and coloured dissolved organic material require material-specific IOPs that can be multiplied by concentrations of these constituents to generate absolute IOP values. In practice, the ability of radiative transfer models to achieve optical closure is often limited by the accuracy of the specific inherent optical properties (IOPs) that are supplied as inputs.

It is not currently possible to measure the separate contributions of phytoplankton and minerals to total particulate IOPs in situ. One method of obtaining material-specific IOPs is to

* Corresponding author.
E-mail addresses: david.mckee@strath.ac.uk (D. McKee), a.cunningham@strath.ac.uk (A. Cunningham).

0272-7714/$ - see front matter © 2006 Elsevier Ltd. All rights reserved.
doi:10.1016/j.ecss.2006.02.010

examine individual algal cultures (Bricaud et al., 1983; Stramski and Morel, 1990; Ahn et al., 1992) and suspensions of purified minerals (Babin and Stramski, 2002, 2004). The question remains, however, of the extent to which these materials in isolation are representative of the natural particle assemblages found in shelf seas. Efforts to derive specific IOPs from natural mixtures of materials are usually based on the quantitative filter pad absorption method (Yentsch, 1962; Mitchell, 1990; Babin et al., 2003a) combined with bleaching of phytoplankton pigments (Kishino et al., 1985; Neumuller et al., 2002) or the removal of organic material by combustion (Bowers et al., 1996). Filter pad measurements may be subject to artefacts due to sample handling (Stramski, 1990; Allali et al., 1995) and there is some uncertainty surrounding optical pathlength amplification at low optical densities (Kiefer and SooHoo, 1982; Mitchell and Kiefer, 1984; Maske and Haardt, 1987; Bricaud and Stramski, 1990; Cleveland and Weidemann, 1993; Roesler, 1998). Laboratory analyses are also time consuming and therefore measurements are temporally and spatially limited compared to in situ methods. Total IOPs have been partitioned into partial components through numerical decomposition (Morrow et al., 1989; Roesler et al., 1989; Bricaud and Stramski, 1990; Cleveland and Perry, 1994; Chang and Dickey, 1999) but this method requires a more accurate knowledge of the spectral characteristics of natural materials than is usually available.

The approach to the problem considered in this paper was to derive useful approximations to material-specific IOPs from a statistical examination of in situ measurements of the total coefficients of absorption, attenuation and backscattering, together with measured concentrations of the most optically significant seawater constituents. The material-specific IOPs obtained by this method were designated effective IOPs because they represented the optical characteristics of natural particle assemblages in the region of interest, dominated by phytoplankton or suspended minerals but containing proportions of other associated materials. A key element of this approach was the identification of optical water types using inter-relationships between IOPs. This sub-classification of Case 2 waters permitted successful regression of particulate IOPs against a single constituent for each optical water type. The resulting effective material-specific IOPs can be used to generate apparent optical properties using established relationships from the literature (Morel and Gentili, 1993), or to parameterise radiative transfer simulations for ecosystem modelling or remote sensing applications.

Coastal waters such as the Irish Sea are optically complex due to variability in constituent concentration and composition. Our methodology for classification of sub-Case 2 optical water types was developed as a means of reducing this complexity by identifying stations where the composition of materials was similar. Attempts to use other classification schemes based on season or geographic location were attempted but were found to be inadequate. Coastal waters such as the Irish Sea exhibit complexity than can be attributed to seasonal, episodic, tidal, geographic and other factors. We believe that our approach may be usefully adapted in other geographical regions and in other areas of optical oceanography, particularly in the interpretation of remote sensing data from coastal waters. In this paper, our purpose was to use this classification scheme to derive material-specific IOPs that could be used for radiative transfer modelling. Whilst the effective mass-specific IOPs we obtained may only be relevant for the Irish Sea (this has yet to be determined), we believe that the methodology we have developed could be successfully exported to other areas.

2. Methods

The Irish Sea, a shallow shelf sea lying between the islands of Ireland and Great Britain, provides a wide range of water types in a relatively small geographical area. It is connected to the North Atlantic through the North Channel and to the Celtic Sea via St Georges Channel. Strong fluctuations in suspended sediment concentrations have been observed in this area (Buchan et al., 1967; Mitchelson, 1984), with tidal currents being the primary source of resuspension activity (Weeks and Simpson, 1991; Bowers et al., 1998). Suspended sediment strongly influences the optical properties of the Irish Sea (Mitchelson et al., 1986; Brown and Simpson, 1990), and an empirical algorithm relating irradiance reflectance to the concentration of mineral suspended solids has been derived (Binding et al., 2003). For this study a total of 98 stations were sampled during a series of cruises between August 2001 and July 2002 at locations shown in Fig. 1. All the data collected for this work came from Case 2 waters where non-algal materials had a significant impact on optical properties.

2.1. IOP measurements

A 25-cm pathlength WET Labs AC-9 was used to measure the absorption coefficient (a_n) and beam attenuation coefficient (c_n) of materials other than water at nine wavelengths (10 nm FWHM) across the visible spectrum. Optical blanks for the AC-9 were regularly measured using ultrapure Millipore water treated with ultraviolet light, and calibration of the two optical channels remained within the manufacturer's specifications of $\pm 0.005\ m^{-1}$. Absorption and attenuation signals at 715 nm were corrected for temperature dependent water absorption (Pegau et al., 1997) and the data were averaged over 1-m depth intervals. Total absorption (a) and attenuation (c) coefficients were obtained by adding partial coefficients for pure water obtained from the literature (Pope and Fry, 1997). Particulate scattering coefficients were obtained from $b_p = c_n - a_n$. Procedures for the correction of in situ reflecting tube absorption measurements for scattering artefacts are still a subject of active discussion (Kirk, 1992; Zaneveld et al., 1994; Piskozub et al., 2001). The Zaneveld et al. (1994) scattering correction was used in this paper, but it may not fully account for the effects of wavelength dependent scattering phase functions in shelf seas (McKee et al., 2003; McKee and Cunningham, 2005). Values of absorption and scattering at 470 nm, used at various points in the paper, were obtained by linear interpolation between AC-9 readings at 440 nm and 488 nm. Total backscattering (b_b) was measured at

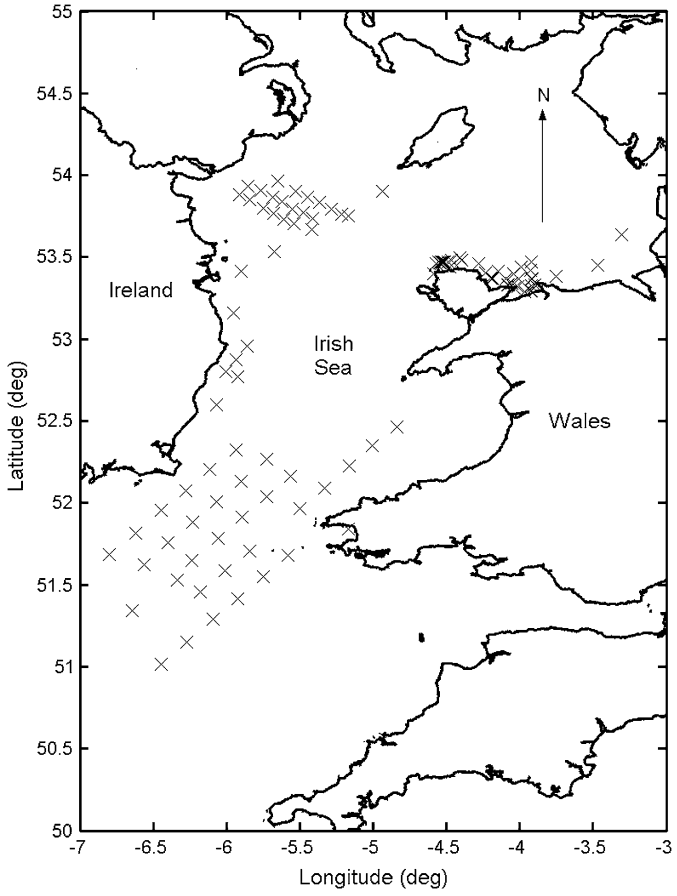

Fig. 1. Map of the Irish Sea indicating the location of 98 stations.

470 nm and 676 nm using a Hydroscat-2 (HOBI Labs). Backscattering signals were corrected for pathlength attenuation effects using the manufacturer's sigma correction procedure. The sigma correction parameter was calculated with a three-term polynomial expansion (coefficients for the polynomial supplied by the manufacturer) on K_{bb}, which in turn was given by $K_{bb} = a + 0.75b$ (see McKee and Cunningham, 2005 for further details). Particulate backscattering (b_{bp}) was obtained by subtracting values for pure water backscattering derived from the measurements of Smith and Baker (1981). It is possible that the 676-nm backscattering channel (with a 20-nm FWHM bandwidth) may be contaminated by fluorescence in waters with high chlorophyll concentrations. Given the limited range of chlorophyll concentration encountered in this Irish Sea data set, and the fact that we could find no obvious feature in the data, we suggest that our backscattering signals at 676 nm may be slightly overestimated for some stations, but it is currently impossible to give an accurate figure for the problem.

2.2. Sample analyses

Chlorophyll samples were filtered through 25-mm GF/F filters and immediately frozen. Once in the laboratory, the filter papers were soaked for 24 h in neutralised 90% acetone and the absorbance of the extract measured in a custom-built spectrophotometer using 1-cm pathlength cuvettes before and after acidification with dilute hydrochloric acid. The trichromatic equations of Jeffrey and Humphrey (1975) were used to convert absorbance spectra to concentrations of chlorophyll *a* (Chl). All samples were measured in triplicate.

Total suspended solids' (TSS) samples were obtained by filtering 5 l of seawater through pre-weighed 90-mm GF/F filters and rinsing with 50 ml of distilled water. Samples were stored frozen until returned to the laboratory where they were dried in an oven at 100 °C for 3 h and reweighed. The concentration of mineral suspended solids (MSS) was obtained by re-weighing samples after they had been placed in a furnace at 500 °C for 3 h, at which point it was assumed that all organic materials had been combusted.

Coloured dissolved organic material (CDOM) samples were filtered through 0.2-μm membrane filters, with the filtrate being collected in acid-rinsed glass bottles with nalgene caps and stored under refrigeration. Absorption by CDOM was measured in a custom-built spectrophotometer using 10-cm cuvettes and UV treated ultrapure water as a reference. Given the unknown and probably complex chemical composition of CDOM, the absorption coefficient of the filtrate material at 440 nm, $a_{CDOM}(440)$, was used as a proxy for concentration of CDOM. Absorption by CDOM samples was subtracted from in situ AC-9 non-water absorption signals, $a_n(\lambda)$, to provide values of particulate absorption, $a_p(\lambda)$.

3. Results

As this paper is primarily concerned with understanding the relationships between IOPs and constituents for radiative transfer modelling of reflectance and euphotic depth, only data from the upper mixed layer were considered. This layer was sampled at a depth of 1 m at all stations. In situ optical measurements are increasingly common, but it is currently difficult to incorporate such data into radiative transfer simulations that extend beyond the limits of the actual data set. Relationships between IOPs and constituents were examined with a view towards determining material-specific IOPs from in situ measurements. Material-specific IOPs derived in this way could be used to model light fields over a much broader range of constituent concentrations than are likely to be obtained even in an extensive sampling campaign such as that undertaken for this study.

3.1. Distributions of seawater constituents

Fig. 2 shows histograms of TSS, MSS, Chl and CDOM for surface samples from 98 stations in the Irish Sea. Both TSS and MSS showed a considerable range of variability. The percentage of TSS due to MSS varied from 20% to 85% with an average of ~60%. The highest levels of both MSS and TSS were found in waters off the north coast of Anglesey and along the north coast of Wales. Despite extensive sampling (three cruises) during spring and summer when phytoplankton populations might be expected to be relatively abundant, more than

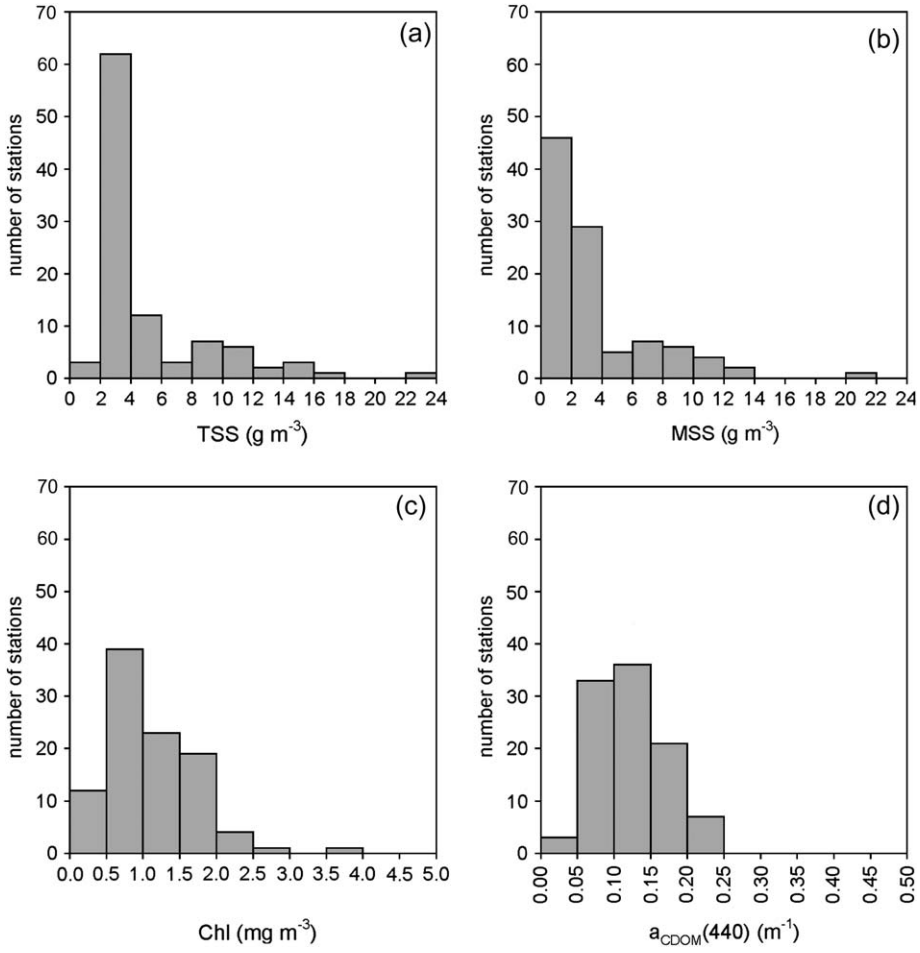

Fig. 2. Histograms of the concentrations of seawater constituents (TSS, MSS, Chl and CDOM) for surface samples from the locations indicated in Fig. 1.

90% of our chlorophyll samples were below 2 mg m^{-3}, and none were greater than 4 mg m^{-3}. High chlorophyll waters may have been inadvertently under-sampled, but it is possible that phytoplankton productivity in these waters is not as high as in other European shelf seas (e.g., Babin et al., 2003a). Chl estimates from satellite imagery are available for the Irish Sea but are unreliable due to the poor performance of standard algorithms in turbid waters. Absorption by CDOM at 440 nm was always less than 0.25 m^{-1} for this data set, even though a number of samples were taken close to outflows of rivers (e.g., in Conwy Bay). These values were low compared to some other UK coastal waters, particularly the fjord systems of the Scottish west coast (McKee et al., 2002), but they were sufficient to ensure that all of these stations could be classed as Case 2.

3.2. IOP distributions

Fig. 3 shows the average spectral dependency of the absorption and scattering coefficients (by all materials other than water) for the entire data set, together with statistical boundaries and histograms of the values observed at 440 nm. The range of variability in the spectral plots was considerable, though the histograms show that ~70% of a_n440 values were below 0.3 m^{-1}, and ~65% of b_p440 values were below 1 m^{-1}. Absorption generally increased exponentially towards the blue end of the spectrum (best-fit exponents were approximately 0.010 nm^{-1} for these spectra) due to the presence of both CDOM and suspended non-algal particles, and there was evidence of a chlorophyll absorption peak at 676 nm. Scattering spectra did not show strong wavelength dependence.

Particulate backscattering distributions (not shown) were very similar to the scattering distribution shown in Fig. 3, with a broad range of variability (<0.001 to ~0.430 m^{-1}) but with 80% of the values below 0.050 m^{-1}. The average particulate backscattering at 440 nm was 0.039 m^{-1}. The wavelength dependency of b_{bp} varied, but was often slightly greater in the blue than in the red (e.g., average $b_{bp}676 = 0.035$ m^{-1}). Backscattering ratios (b_b/b) varied over an order of magnitude from ~0.005 to ~0.050, with average values of 0.025 at 470 nm and 0.020 at 676 nm. This range of values was consistent with those of Petzold (1972) who found backscattering ratios of 0.019 for turbid waters in San Diego harbour, and 0.013 for coastal ocean waters. Petzold also found a backscattering ratio of 0.044 for clear open ocean waters. In those waters a high backscattering ratio probably arose as a result of the diminishing importance of particulate scattering relative to molecular scattering by

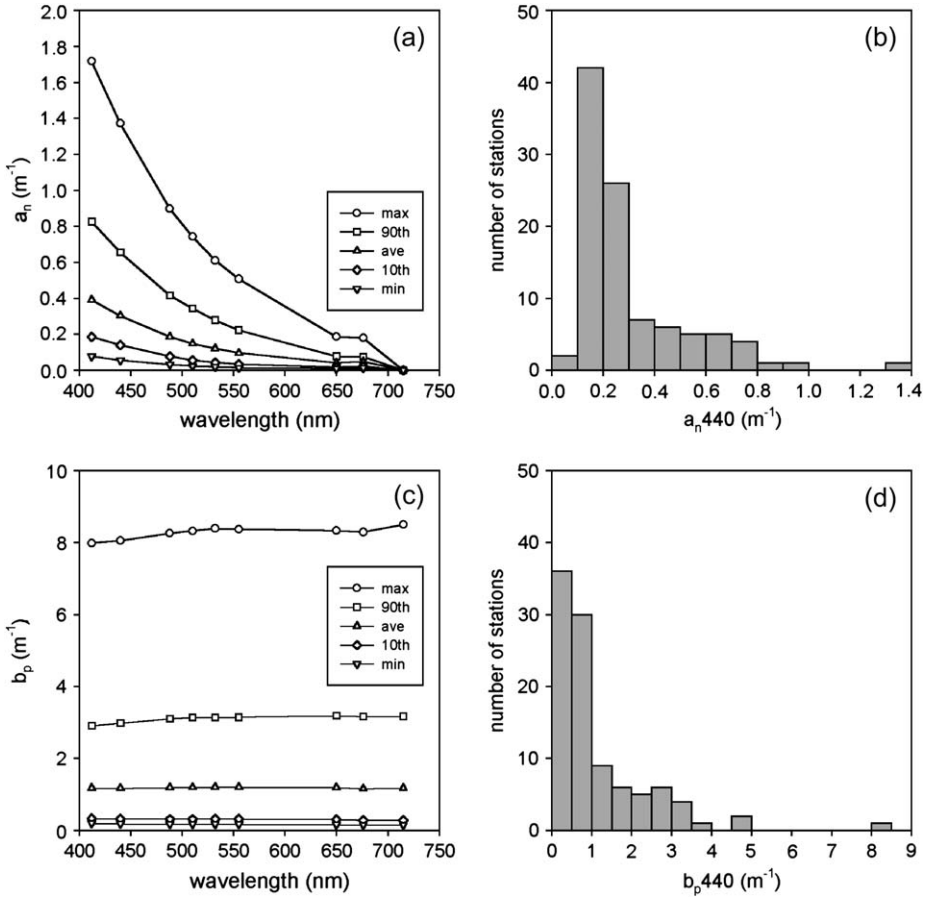

Fig. 3. Spectral characteristics and distributions of values at 440 nm for the absorption and scattering coefficients of materials other than water in the Irish Sea data set. Panels (a) and (c) show mean values of the absorption and scattering coefficients together with maxima, minima and the 10th and 90th percentile points for each wavelength.

seawater ($b_b/b = 0.5$ for pure seawater). This should not be confused with high backscattering ratios for turbid waters, such as those reported here, which are probably due to the presence of highly scattering mineral particles.

3.3. Inter-relationships between IOPs

Fig. 4a shows particulate backscattering (b_{bp}) plotted against absorption by materials other than water (a_n) at 676 nm for surface waters in the Irish Sea. The data were divided into two clusters by drawing a line through the origin with a gradient $b_{bp}/a_n = 0.33$. The branch with higher values of b_{bp} was termed 'Group A' and the lower b_{bp} branch was termed 'Group B'. Fig. 4b and c shows that Group A stations had higher blue (440 nm) to red (676 nm) absorption ratios and also higher ratios of scattering to absorption at 676 nm. Fig. 4d shows distributions of particulate backscattering ratios (b_{bp}/b_p) at 470 nm for the Group A and Group B subsets. The particulate backscattering ratio was generally low (0.005–0.030) for Group B stations, and generally high (0.015–0.055) for Group A stations. McKee and Cunningham (2005) introduced the parameter B, defined as

$$B = \frac{(b_b/b)_{470}}{(b_b/b)_{676}} \quad (1)$$

to quantify wavelength dependence of the scattering phase function. A plot of B against the ratio of b_{bp}/a_n at 676 nm (Fig. 5) shows that the strongest wavelength dependency was observed for low values of b_{bp}/a_n and that the wavelength dependence was relatively uniform and low (average $B = 1.15$) for Group A data. This suggests that the scattering phase function shows greater and more variable wavelength dependence in waters where phytoplankton dominate particulate IOPs, and that there is less variability and lower wavelength dependence in waters where minerals dominate.

3.4. Relationships between IOPs and constituents

Linear regression analysis, applied independently to the two data subsets, indicated that particulate IOPs for Group A stations were largely driven by variations in concentrations of MSS, while most of the variability observed for Group B stations was attributable to changes in Chl. (Note: particulate absorption was derived from in situ absorption by subtracting the component due to CDOM.) For example, Fig. 6 shows the

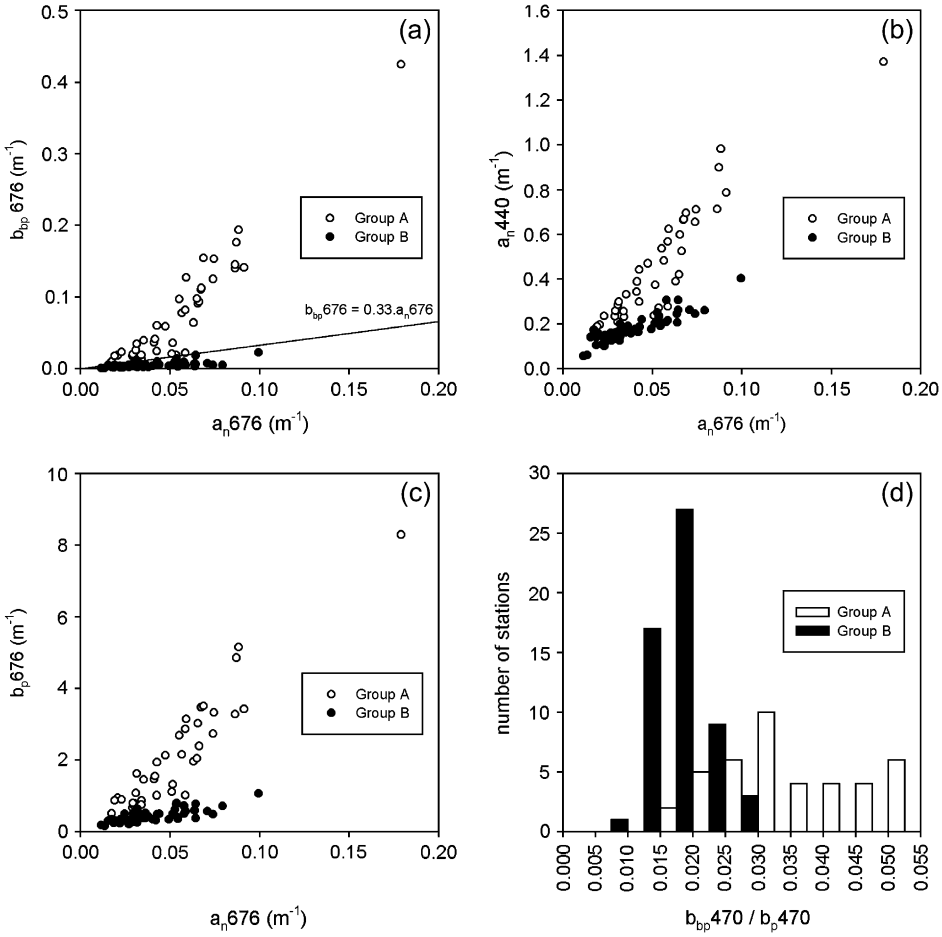

Fig. 4. Data from the Irish Sea form distinct clusters in plots of (a) particulate backscattering against non-water absorption at 676 nm, (b) non-water absorption at 440 nm and 676 nm and (c) particulate scattering at 676 nm against non-water absorption at 676 nm. Filled and open symbols designate points that were classified as Group A and Group B using the line drawn in panel (a). The particulate backscattering ratio at 470 nm (d) is lower for Group B stations than for Group A stations.

particulate absorption coefficient at 440 nm, the particulate scattering coefficient at 555 nm and the particulate backscattering coefficient at 676 nm plotted against MSS for Group A stations, and against Chl for Group B stations. MSS typically accounted for between 85% and 95% of the observed variability in all IOPs for Group A stations, with the exception of absorption at 650 nm and 676 nm where the figures drop to 83% and 76%, respectively. For Group B stations the degree of variability accounted for by Chl was typically less than 40%, though it rose to almost 60% for absorption at 676 nm. The relationships for the Group B group were statistically significant (e.g., $t > 10$, $p < 0.001$, $n = 57$ in all cases) and no significant improvement in the degree of variability accounted for was obtained by multiple linear regression on both Chl and MSS. Regression lines (forced through the origin) like those shown in Fig. 6 were calculated for all AC-9 wavebands. The coefficients for the two data groups then provided effective material-specific IOPs for chlorophyll-dominated and sediment-dominated waters. In this procedure the IOPs have not been completely partitioned into Chl-specific and MSS-specific contributions. Rather, the regression analysis indicated that Chl had a minimal influence on IOPs for Group A data,

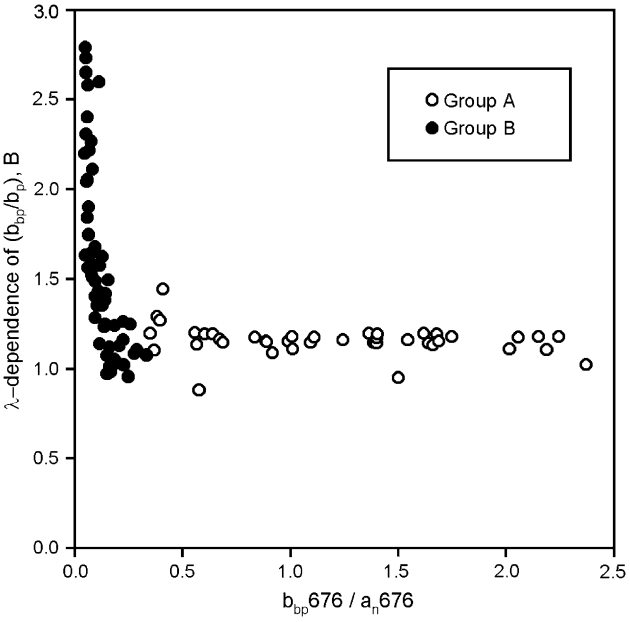

Fig. 5. Group B stations show much stronger wavelength dependence in the particulate backscattering ratio (higher *B*) than Group A stations, indicating suspended particle assemblages with significantly different optical properties.

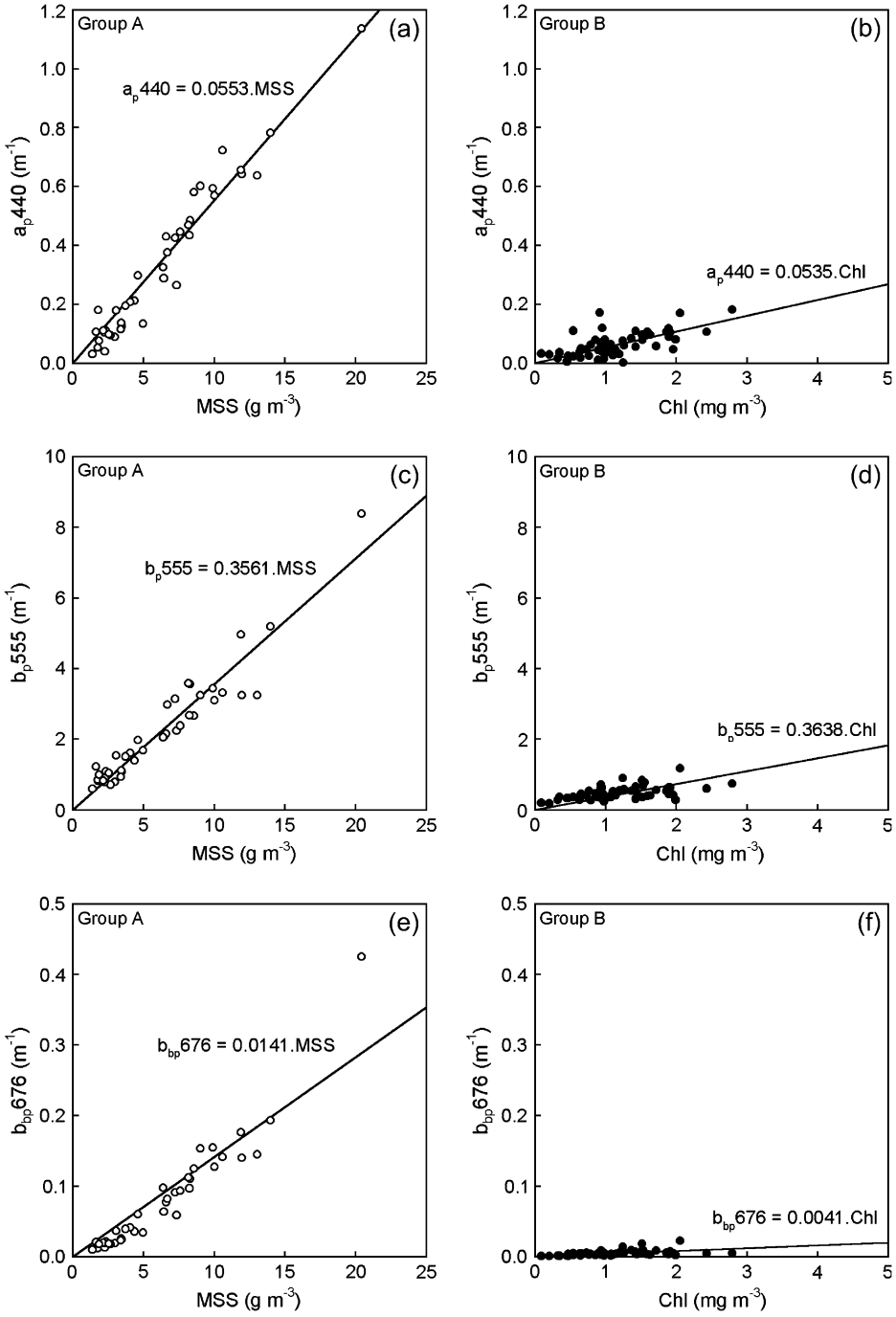

Fig. 6. Results of linear regression analyses for the segregated data set. IOPs from Group A stations correlate well with MSS while IOPs from Group B stations can be correlated with Chl. The equations displayed are for best-fit lines forced through the origin.

while the effect of MSS could be neglected for Group B stations. In order to distinguish 'effective' material-specific IOPs from 'true' values they were denoted by $a^{+}(\lambda)$ etc. rather than the normal $a^{*}(\lambda)$. Fig. 7 shows effective material-specific absorption and scattering spectra (with 95% confidence intervals) for Group A and Group B stations. The a^{+}_{MSS} spectrum for Group A stations (Fig. 7a) increased exponentially into the blue as expected for mineral rich waters, with a small residual chlorophyll absorption peak at 676 nm. The b^{+}_{MSS} spectrum for Group A stations (Fig. 7b) was relatively flat with wavelength, with a very slight decrease towards shorter wavelengths. Fig. 7d indicates that effective chlorophyll-specific scattering (b^{+}_{Chl}) for Group B stations was also only slightly wavelength dependent, though in this case the decrease was towards longer wavelengths. Finally, the ratio of blue to red absorption in the a^{+}_{Chl} spectrum shown in Fig. 7c was slightly higher than expected, probably due to residual absorption by detrital materials in these measurements. Numerical values for effective material-specific particulate backscattering coefficients are given in Table 1 for both Group A and Group B

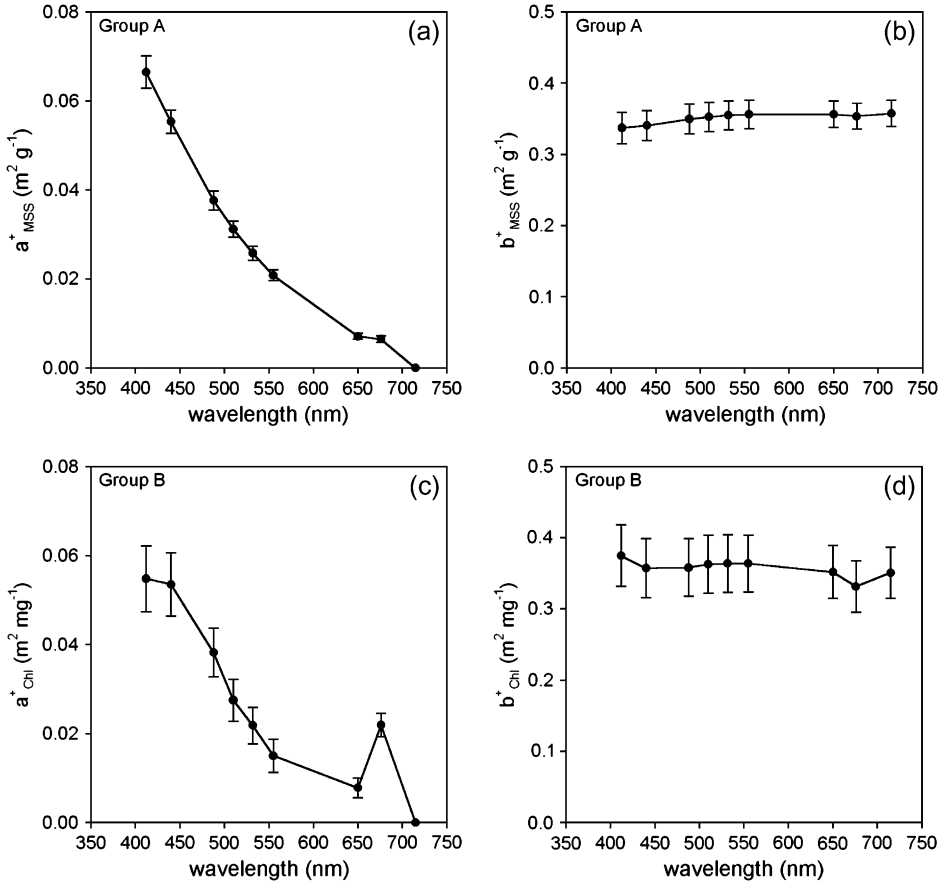

Fig. 7. Spectral values of effective material-specific absorption and scattering coefficients for Group A and Group B subsets derived using linear regression coefficients. The bars indicate 95% confidence intervals.

subsets. In both cases the effective specific particulate backscattering was slightly higher in the blue than in the red. Numerical values of the effective material-specific absorption and scattering coefficients are given in Table 2.

3.5. A method for estimating Irish Sea IOPs from constituents

One application for the effective material-specific IOPs derived above would be for the estimation of total IOPs from data sets containing only constituent information (Chl, MSS and CDOM). Before this can be done, however, we need to determine the quality of the material-specific IOPs and a means of identifying water types from constituents. The merit of these effective material-specific IOPs can be partially assessed in terms of their self-consistency when used in a model for estimating total IOPs from the analysis of seawater constituents. In the absence of backscattering and absorption measurements, the water has to be categorised as Group A or Group B (or equivalents) using the constituent concentrations themselves. Since the ratio of Chl/MSS was lower than 0.4 mg g^{-1} for 93% of the Group A stations and above 0.4 mg g^{-1} for 86% of the Group B stations, Chl/MSS = 0.4 mg g^{-1} was found to be an optimal threshold for discriminating between Group A and Group B waters for this data set. Particulate IOPs were calculated using the material-specific IOPs derived previously together with measured values of either MSS or Chl depending on whether a station had been classed as group A or B using the Chl/MSS threshold. The absorption by CDOM was calculated using

$$a_{\mathrm{CDOM}}(\lambda) = a'_{\mathrm{CDOM}}(440)\left[\mathrm{e}^{(-0.014(\lambda-440))} - \mathrm{e}^{(-0.014(715-440))}\right], \quad (2)$$

where a'_{CDOM} was the measured absorption by CDOM at 440 nm and the second term inside the square brackets ensured that absorption by CDOM at 715 nm was zero. This was necessary for compatibility with AC-9 measurements. The exponent of 0.014 nm^{-1} is widely used and reasonably typical of these waters: our observed values lie in the range of

Table 1
Effective material-specific particulate backscattering coefficients (with 95% confidence intervals) for Group A and Group B subsets derived from linear regressions

	Group A	Group B
	$b^+_{\mathrm{bp\,MSS}}$ (m^2 g^{-1})	$b^+_{\mathrm{bp\,Chl}}$ (m^2 mg^{-1})
470 nm	0.0152 ± 0.0011	0.0050 ± 0.0009
676 nm	0.0141 ± 0.0013	0.0041 ± 0.0007

Table 2
Effective material-specific particulate absorption and scattering coefficients (with 95% confidence intervals) for Group A and Group B subsets derived from linear regressions

	Group A		Group B	
	a^{+}_{MSS} ($m^2\,g^{-1}$)	b^{+}_{MSS} ($m^2\,g^{-1}$)	a^{+}_{Chl} ($m^2\,mg^{-1}$)	b^{+}_{Chl} ($m^2\,mg^{-1}$)
412 nm	0.0665 ± 0.0036	0.3372 ± 0.0221	0.0548 ± 0.0074	0.3748 ± 0.0431
440 nm	0.0553 ± 0.0026	0.3404 ± 0.0212	0.0535 ± 0.0071	0.3573 ± 0.0414
488 nm	0.0376 ± 0.0021	0.3496 ± 0.0208	0.0382 ± 0.0055	0.3581 ± 0.0406
510 nm	0.0312 ± 0.0018	0.3524 ± 0.0205	0.0275 ± 0.0047	0.3628 ± 0.0410
532 nm	0.0258 ± 0.0016	0.3547 ± 0.0203	0.0218 ± 0.0041	0.3639 ± 0.0406
555 nm	0.0208 ± 0.0012	0.3561 ± 0.0198	0.0150 ± 0.0037	0.3638 ± 0.0399
650 nm	0.0071 ± 0.0007	0.3563 ± 0.0183	0.0078 ± 0.0022	0.3519 ± 0.0373
676 nm	0.0065 ± 0.0007	0.3534 ± 0.0182	0.0219 ± 0.0026	0.3314 ± 0.0361
715 nm	0	0.3575 ± 0.0183	0	0.3508 ± 0.0360

$0.009-0.019\ nm^{-1}$ with a mode of $0.013\ nm^{-1}$. Calculated IOPs did not include water, and calculated absorption values included both dissolved and particulate components. Fig. 8 shows calculated IOPs plotted against in situ measurements for the entire data set and for all available wavelengths. Best-fit lines through the data have slopes reasonably close to unity, low offsets and regression coefficients between 0.9 and 0.96, indicating very satisfactory overall performance.

3.6. Modelled remote sensing reflectance for two Irish Sea optical water types

Remote sensing reflectance is strongly influenced by both absorption and backscattering (see below). Previously we have identified two optical water types that could be distinguished from the ratio of particulate backscattering to non-water absorption at 676 nm. It would be of considerable interest if these two optical water types could also be distinguished from their reflectance properties.

Morel and Gentili (1993) showed that the remote sensing reflectance immediately beneath the sea surface, R_{rs}, was related to the ratio of backscattering to absorption via

$$R_{rs} = \frac{f}{Q}\frac{b_b}{a} \tag{3}$$

where Q is the ratio of upwards irradiance to radiance (E_u/L_u) and f is a coefficient that varies with solar angle and the optical properties of the seawater. In their analysis, Morel and Gentili demonstrated that f/Q varied over a limited range of values for solar angles appropriate for remote sensing applications. For wavelengths in the blue and green, a value of $f/Q \approx 0.095$ was found to have the most common occurrence. Remote sensing reflectance at 555 nm was calculated from measured concentrations of seawater constituents for each point in the Irish Sea data set using

$$R_{rs} = 0.095\left(\frac{b_{bw} + b_{bp}}{a_w + a_p + a_{CDOM}}\right) \tag{4}$$

with the IOPs having been calculated using the procedure outlined in Section 3.5 (i.e., using effective material-specific IOPs from Tables 1 and 2 for each optical water type) and with pure water IOPs being derived from the measurements of Pope and Fry (1997) and Smith and Baker (1981). Fig. 9 shows the distribution of modelled values of R_{rs} at 555 nm for the Irish Sea data set segregated by optical water type. The data set was cleanly split between stations with Chl/MSS $> 0.4\ mg\,g^{-1}$ that had low values of b_b/a and correspondingly low sub-surface remote sensing reflectances ($\leq 0.015\ sr^{-1}$), and stations with Chl/MSS $> 0.4\ mg\,g^{-1}$ that had values of $R_{rs} > 0.015\ sr^{-1}$. Modelled reflectances were generally higher across all wavelengths for stations with low Chl/MSS and hence high b_b/a. This result suggests that it may be possible to distinguish these optical water types from space using the magnitude of remote sensing reflectance signals.

4. Discussion

This Irish Sea data set contained two Case 2 water sub-types that could be distinguished optically (using the ratio of particulate backscattering to non-water absorption at 676 nm) or by the ratio of the concentrations of their constituents (Chl/MSS). Stations with high values of b_{bp}/a_n (Group A) had low ratios of chlorophyll a to suspended minerals, while stations with low levels of b_{bp}/a_n (Group B) had higher ratios. Regression analysis demonstrated that the particulate IOPs of Group A stations were highly correlated with the concentration of suspended minerals, while those for Group B stations were largely determined by phytoplankton. 'Effective' material-specific particulate IOPs for the two data subsets were determined by linear regression. Note that although the particulate IOPs were dominated by phytoplankton for Group B stations, the presence of significant levels of CDOM affected total absorption signals and therefore this group of data would have to be classified as a Case 2 sub-type rather than Case 1. To the best of our knowledge this is the first published attempt to use IOP relationships to segregate sub-groups of Case 2 waters, enabling estimation of effective specific IOPs from in situ measurements of total IOPs. The derived relationships allow total IOPs to be estimated from measurements of seawater constituents. They provide a basis for assimilating routine water-quality observations in radiative transfer models and validating products from ocean colour sensors in regions where programs of water sample analyses

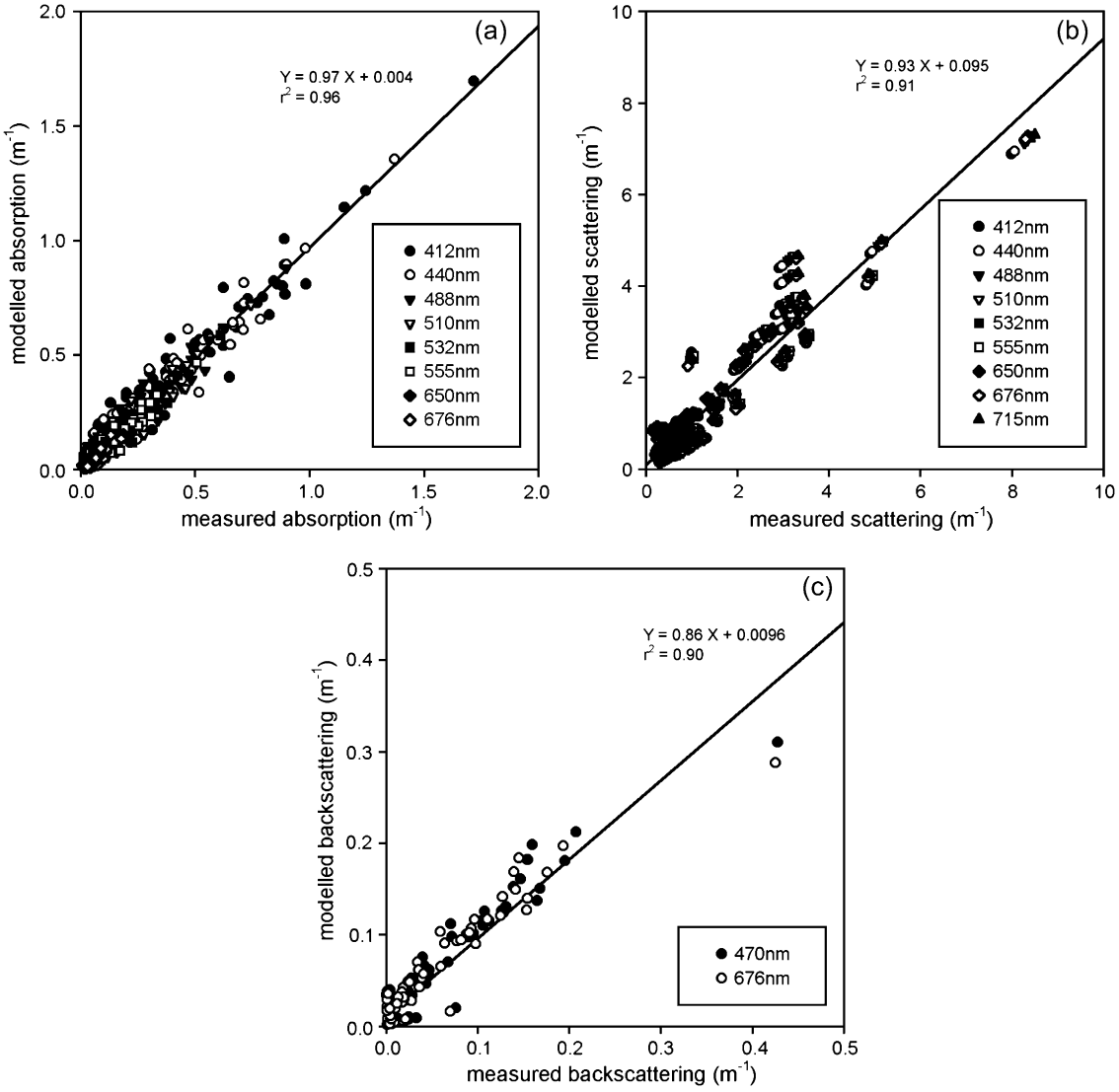

Fig. 8. IOPs modelled using effective material-specific IOPs from Tables 1 and 2 and a threshold Chl/MSS value of 0.4 mg g^{-1} to determine water type show very good agreement with in situ measurements.

are routinely carried out but simultaneous optical measurements may not be available. The process of identifying optical water types from IOP relationships may be extended to other geographical regions with different optical properties.

'Effective' specific IOPs were conceived as modelling tools, but their relationship to true specific IOPs for the two main particle types could be assessed using values from the literature. For the Group B case, the chlorophyll-specific absorption coefficients of 0.054 and 0.022 $m^2\,mg^{-1}$ at 440 nm and 676 nm, respectively, were close to the centres of the ranges (0.015–0.127 and 0.01–0.035 $m^2\,mg^{-1}$) measured by Ahn et al. (1992) for nine different algal cultures, and within the range observed by Babin et al. (2003a) for other European coastal waters. Our value of $b^{+}_{Chl}(555) = 0.364\ m^2\,mg^{-1}$ was slightly higher than the range of 0.023–0.307 $m^2\,mg^{-1}$ observed by Ahn et al., while our chlorophyll-specific backscattering coefficient was roughly four times higher than the maximum value of $0.99 \times 10^{-3}\ m^2\,mg^{-1}$ determined by these authors. It is likely that these discrepancies in chlorophyll-specific scattering and backscattering are caused by the presence of higher concentrations of small particles (detritus, bacteria, small inorganic particles) in natural samples than in algal cultures. It was more difficult to evaluate the material-specific optical coefficients from Group A waters because of inconsistencies in the methods adopted by different sources, such as the use of TSS (or SPM) rather than MSS, and variations in the techniques used to eliminate the phytoplankton component of absorption. For example, other authors have used the subscript 'min' to denote 'mineral' where we have used 'MSS' to denote the use of mineral suspended solids in the calculation of each material-specific IOP. Bowers et al. (1996) found an average value of $a^*_{min}(440)$ of $\sim 0.10\ m^2\,g^{-1}$ for inorganic particles from the Irish Sea, Babin and Stramski (2004) give values of $a^*_{min}(443)$ ranging between 0.03 and 0.10 $m^2\,g^{-1}$ for various minerals suspended in water, and Babin et al. (2003a) found an average value of 0.041 $m^2\,g^{-1}$ for

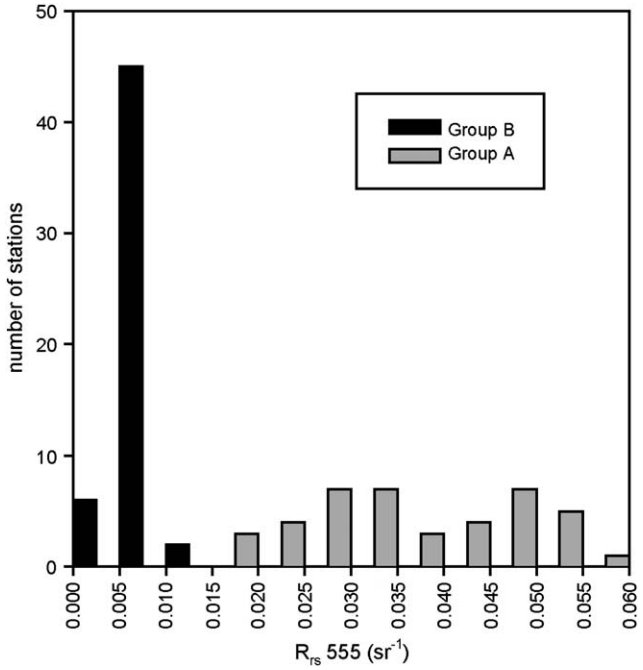

Fig. 9. Modelled remote sensing reflectances are higher for stations where mineral particles most strongly influence particulate IOPs (Group A) than for stations where phytoplankton are the key particulate material (Group B).

European coastal waters. We found a best-fit value for $a^{+}_{MSS}(440)$ of 0.055 $m^2\,g^{-1}$ for Group A stations which lies close to the centre of the Babin and Stramski range and agrees well with the Babin et al. average value, but is lower than the Bowers et al. value. Our b^{+}_{MSS} value of $\sim$0.35 $m^2\,g^{-1}$ for Group A waters is lower than the range of 0.8–1.5 $m^2\,g^{-1}$ measured by Stramski et al. (2004) for Asian mineral dusts suspended in seawater but is closer to the average values reported by Babin et al. (2003b) for European coastal waters (0.42–0.56 $m^2\,g^{-1}$).

5. Conclusion

In the case of the Irish Sea, the occurrence of distinct water types is not an artefact of the distribution of sampling effort: it can be linked to physical mechanisms. Suspended mineral concentrations are elevated over the whole region during the winter months and in regions of high tidal stirring throughout the year (Bowers et al., 1998), and it is likely that the Group A water type occurs when these elevated mineral levels are not accompanied by significant phytoplankton populations. Conversely, Group B waters are expected in areas where the water column stratifies in spring and summer, suspended minerals sediment out, and phytoplankton growth occurs. In spite of extensive sampling over four cruises, we have not encountered simultaneously high concentrations of phytoplankton and minerals in the Irish Sea. Our preliminary modelling indicates that the composition of the particulate population may have a significant impact on the magnitude of R_{rs} signals. The incorporation of the effective material-specific IOPs derived in this paper in radiative transfer simulations, and comparison of the results with satellite measurements of water-leaving radiance, will form the basis of future work.

References

Ahn, Y., Bricaud, A., Morel, A., 1992. Light backscattering efficiency and related properties of some phytoplankters. Deep Sea Research 39, 1835–1855.

Allali, K., Bricaud, A., Babin, M., Morel, A., Chang, P., 1995. A new method for measuring spectral absorption coefficients of marine particles. Limnology and Oceanography 40, 1526–1532.

Babin, M., Stramski, D., 2002. Light absorption by aquatic particles in the near-infrared spectral region. Limnology and Oceanography 47, 911–915.

Babin, M., Stramski, D., Ferrari, G.M., Claustre, H., Bricaud, A., Obolensky, G., Hoepffner, N., 2003a. Variations in the light absorption coefficients of phytoplankton, nonalgal particles, and dissolved organic matter in coastal waters around Europe. Journal of Geophysical Research 108 (C7), 3211. doi:10.1029/2001JC000882.

Babin, M., Morel, A., Fournier-Sicre, V., Fell, F., Stramski, D., 2003b. Light scattering properties of marine particles in coastal and open ocean waters as related to the particle mass concentration. Limnology and Oceanography 48, 843–859.

Babin, M., Stramski, D., 2004. Variations in the mass-specific absorption coefficient of mineral particles suspended in water. Limnology and Oceanography 49, 756–767.

Binding, C.E., Bowers, D.G., Mitchelson-Jacob, E.G., 2003. An algorithm for the retrieval of suspended sediment concentrations in the Irish Sea from SeaWiFS ocean colour satellite imagery. International Journal of Remote Sensing 24, 3791–3806.

Bowers, D.G., Harker, G.E.L., Stephan, B., 1996. Absorption spectra of inorganic particles in the Irish Sea and their relevance to remote sensing of chlorophyll. International Journal of Remote Sensing 17, 2449–2460.

Bowers, D.G., Boudjelas, S., Harker, G.E.L., 1998. The distribution of fine suspended sediments in the surface waters of the Irish Sea and its relation to tidal stirring. International Journal of Remote Sensing 19, 2789–2805.

Bricaud, A., Morel, A., Prieur, L., 1983. Optical efficiency factors of some phytoplankters. Limnology and Oceanography 28, 816–832.

Bricaud, A., Stramski, D., 1990. Spectral absorption coefficients of living phytoplankton and non-algal biogenous matter: a comparison between the Peru upwelling area and the Sargasso Sea. Limnology and Oceanography 35, 562–582.

Brown, J., Simpson, J.H., 1990. The radiometric determination of total pigment and seston and its potential use in shelf seas. Estuarine, Coastal and Shelf Science 31, 1–9.

Buchan, S., Floodgate, G.D., Crisp, D.J., 1967. Studies on the seasonal variation of the suspended matter of the Menai Strait: II. The inorganic fraction. Limnology and Oceanography 12, 419–431.

Bulgarelli, B., Zibordi, G., Berthon, J.F., 2003. Measured and modeled radiometric quantities in coastal waters: towards a closure. Applied Optics 42, 5365–5381.

Chang, G.C., Dickey, T.D., 1999. Partitioning in situ total spectral absorption by use of moored spectral absorption–attenuation meters. Applied Optics 38, 3876–3887.

Chang, G.C., Dickey, T.D., Mobley, C.D., Boss, E., Pegau, W.S., 2003. Toward closure of upwelling radiance in coastal waters. Applied Optics 42, 1574–1582.

Cleveland, J.S., Weidemann, A.D., 1993. Quantifying absorption by aquatic particles: a multiple scattering correction for glass-fiber filters. Limnology and Oceanography 38, 1321–1327.

Cleveland, J.S., Perry, M.J., 1994. A model for partitioning particulate absorption into phytoplanktonic and detrital components. Deep Sea Research I 41, 197–221.

Jeffrey, S.W., Humphrey, G.F., 1975. New spectrophotometric equations for determining chlorophylls *a*, *b*, c_1 and c_2 in higher plants, algae and natural phytoplankton. Biochemie und Physiologie der Pflanzen 167, 191–194.

Kiefer, D.A., SooHoo, J.B., 1982. Spectral absorption by marine particles of coastal waters of Baja California. Limnology and Oceanography 27, 492–499.

Kirk, J.T.O., 1981. Monte Carlo procedure for simulating the penetration of light into natural waters. CSIRO Australian Division of Plant Industry Technical Paper No. 36, 1–16.

Kirk, J.T.O., 1992. Monte Carlo modelling of the performance of a reflective tube absorption meter. Applied Optics 31, 6463–6468.

Kishino, M., Takahashi, M., Okami, N., Ichimura, S., 1985. Estimation of the spectral absorption coefficients of phytoplankton in the sea. Limnology and Oceanography 27, 492–499.

Maske, H., Haardt, H., 1987. Quantitative in vivo absorption spectra of phytoplankton; detrital absorption and comparison with fluorescence excitation spectra. Limnology and Oceanography 32, 620–633.

McKee, D., Cunningham, A., Jones, K.J., 2002. Optical and hydrographic consequences of freshwater run-off during spring phytoplankton growth in a Scottish fjord. Journal of Plankton Research 24, 1163–1171.

McKee, D., Cunningham, A., Craig, S., 2003. Semi-empirical correction algorithm for AC-9 measurements in a coccolithophore bloom. Applied Optics 42, 4369–4373.

McKee, D., Cunningham, A., 2005. Evidence for wavelength dependence of the scattering phase function and its implication for modelling radiance transfer in shelf seas. Applied Optics 44, 126–135.

Mitchell, B.G., 1990. Algorithms for determining the absorption coefficient of aquatic particulates using the quantitative filter technique (QFT). In: Ocean Optics X. Proceedings of SPIE, vol. 1302, pp. 137–148.

Mitchell, B.G., Kiefer, D.A., 1984. Determination of absorption and fluorescence excitation spectra for phytoplankton. In: Holm-Hansen, O., Bolis, L., Gilles, R. (Eds.), Marine Phytoplankton and Productivity. Springer-Verlag, Berlin, New York.

Mitchelson, E.G., 1984. Phytoplankton and suspended sediment distributions in relation to physical structure and water-leaving signals. PhD thesis, University of Wales, Bangor, U.K., unpublished.

Mitchelson, E.G., Jacob, N.J., Simpson, J.H., 1986. Ocean colour algorithms from the case 2 waters of the Irish Sea in comparison to algorithms from case 1 waters. Continental Shelf Research 5, 403–415.

Mobley, C.D., 1994. Light and Water; Radiative Transfer in Natural Waters. Academic, San Diego.

Morel, A., Gentili, B., 1993. Diffuse reflectance of oceanic waters. II. Bidirectional aspects. Applied Optics 32, 6864–6879.

Morrow, J.H., Chamberlin, W.S., Kiefer, D.A., 1989. A two-component description of spectral absorption by marine particles. Limnology and Oceanography 34, 1500–1509.

Neumuller, M., Cunningham, A., McKee, D., 2002. Assessment of a microscopic photobleaching technique for measuring the spectral absorption efficiency of individual phytoplankton cells. Journal of Plankton Research 24, 741–746.

Pegau, W.S., Gray, D., Zaneveld, J.R.V., 1997. Absorption and attenuation of visible and near-infrared light in water: dependence on temperature and salinity. Applied Optics 36, 6035–6046.

Petzold, T.J., 1972. Volume scattering functions for selected ocean waters. SIO Reference Series. Scripps Institution of Oceanography Ref. 72–78. In: Tyler, J.E. (Ed.), Light in the Sea. Dowden, Hutchinson & Ross, Stroudsberg, 1977, pp. 150–174, 79 pp. (Chapter 12).

Piskozub, J., Flatau, P.J., Zaneveld, J.R.V., 2001. Monte Carlo study of the scattering error of a quartz reflective absorption tube. Journal of Atmospheric and Oceanic Technology 18, 438–445.

Pope, R.M., Fry, E.S., 1997. Absorption spectrum (380–700 nm) of pure water. II. Integrating cavity measurements. Applied Optics 36, 8710–8723.

Roesler, C.S., 1998. Theoretical and experimental approaches to improve the accuracy of particulate absorption coefficients derived from the quantitative filter technique. Limnology and Oceanography 43, 1649–1660.

Roesler, C.S., Perry, M.J., Carder, K.L., 1989. Modelling in situ phytoplankton absorption from total absorption spectra in productive inland waters. Limnology and Oceanography 34, 1510–1523.

Sathe, P.V., Sathyendranath, S., 1992. A fortran-77 program for Monte Carlo simulation of upwelling light from the sea. Computers and Geosciences 18, 487–507.

Sathyendranath, S., Prieur, L., Morel, A., 1989. A three-component model of ocean colour and its application to remote sensing of phytoplankton pigments in coastal waters. International Journal of Remote Sensing 10, 1373–1394.

Smith, R.C., Baker, K., 1981. Optical properties of the clearest natural waters (200–800 nm). Applied Optics 20, 177–184.

Smith, R.C., Prézelin, B.B., Bidigare, R.R., Baker, K.S., 1989. Bio-optical modelling of photosynthetic production in coastal waters. Limnology and Oceanography 34, 1524–1544.

Stramski, D., 1990. Artifacts in measuring absorption spectra of phytoplankton collected on a filter. Limnology and Oceanography 35, 1804–1809.

Stramski, D., Morel, A., 1990. Optical properties of photosynthetic picoplankton in different physiological states as affected by growth irradiance. Deep Sea Research 37, 245–266.

Stramski, D., Woźniak, S.B., Flatau, P.J., 2004. Optical properties of Asian mineral dust suspended in seawater. Limnology and Oceanography 49, 749–755.

Weeks, A.R., Simpson, J.H., 1991. The measurement of suspended particulate concentrations from remotely-sensed data. International Journal of Remote Sensing 12, 725–737.

Yentsch, C.S., 1962. Measurement of visible light absorption by particulate matter in the ocean. Limnology and Oceanography 7, 207–217.

Zaneveld, J.R.V., Kitchen, J.C., Moore, C., 1994. The scattering error correction of reflecting-tube absorption meters. In: Jaffe, J.S. (Ed.), Proceedings of Ocean Optics XII, vol. 2258. SPIE, pp. 44–55.